A Novel Investigation of the Design of Experiments on Pakistani Wood Biochar and the Impact of Process Constraints on Biochar's Characteristics

[1]Kalsoom Sarwar*, [1]Zill-i-Huma Nazli**, [2]Hassan Munir, [1]Maryam Aslam, [1]Nusrat Shafiq
[1] *Government College Women University, Faisalabad, Pakistan.*
[2] *University of Agriculture,* Faisalabad, Pakistan.
Kalsoom_sarwar@yahoo.com*

(Received on 14th December 2023, accepted in revised form 21st March 2025)

Summary: Samples of native Pakistani wood looked into as possible locally obtained raw materials for the manufacturing of biochar. The best feedstock found to be pure softwood through screening studies. Using design of experiments, the effects of operating factors, such as flow rate of activating gas (CO_2), contact time and heating ramp rate on ultimate biochar properties studied. The response variables that chosen were surface area and biochar yield. The experimental run conditions were determined using Minitab, which also recommended an ideal output of 60 minutes of contact time and a 17 °C/min ramp rate for maximal reactions. Softwood produced the largest surface area (744 m^2/g) at 850 °C, despite a 13% yield. The observed surface area, with a yield of approximately 16%, was 593 m^2/g under optimal conditions. Pareto charts, which showed a strong correlation with experimental data, indicated that the chosen answers were unaffected by the gas flow rate. The pore structure consisted of a blend of meso and micro pores, with an average point of zero charge of 7.20 ± 0.01 and pore diameters of 2-6 nm. According to proximate analysis, the optimized biochar fixed carbon content increased from 20% in the feedstock to 80%. The biochar's multilayer carbon structure revealed via morphological investigation. The findings demonstrate the importance of the chosen feedstock as a possible basis of biochar material as well as the significance of the interaction between effective variables and their ultimate properties in the formation of biochar.

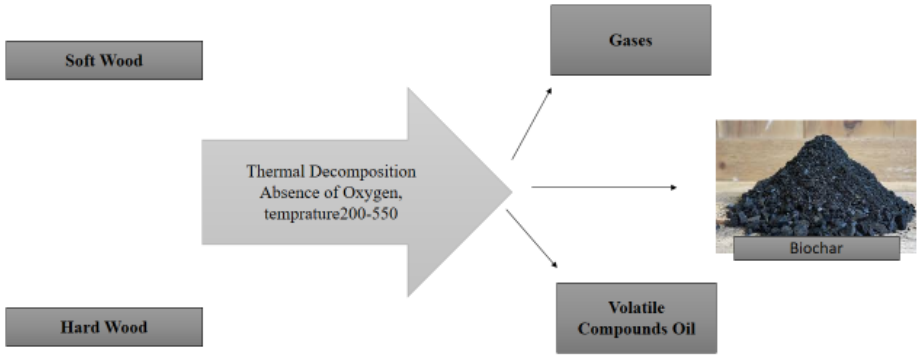

Keywords: Biochar, Pakistani wood, Activated carbon and Pyrolysis.

Introduction

The black carbonaceous residue known as "biochar" created when biomass is converted thermochemically in an inert atmosphere. It acts as a barrier to keep carbon dioxide inside the material instead of releasing it during the organic matters natural breakdown and contributing to greenhouse gas emissions [1]. The combination of inexpensive feedstock availability and a variety of physical and chemical properties allows these materials to function similarly or better than commercially available activated carbons in a variety of applications. This means that carbon-rich biochar has the potential to use in a variety of applications, comprising soil amendments like amelioration fertilizers, energy storage, Nano adsorbents and catalysts [2]. There has been a push recently to generate biochar from renewable sources, adding value to waste streams, as part of the circular economy; however, production is currently unregulated. The manufacturing of biochar, in particular, offers the possibility of ad hoc production and product customization to meet specific application needs. Customized materials that derive from renewable resources and possess properties similar to those of commercially available activated carbons have the potential to aid in lowering the overall carbon footprint of various industrial processes [3].

*To whom all correspondence should be addressed.

Biochar is well suited for adsorption because of their high surface areas and toned pore grids, which range from micro to macro pores. Heavy metals that readily sorb both inside the pore network and on its surface have active binding sites recognitions to the pore network, which permeates the entire substance [4]. Despite having much lower surface area, biochar derived from renewable resources have adsorption capabilities that are comparable to those of commercial activated carbons. These qualities have led to the usage of biochar made from various feedstocks in water treatment applications. For instance, rice husk-based biochar used in catalysis of acid [5], biochar made from paralyzed hard wood have capability uses in the fabrication of biodiesel [6] and when utilized as a soil enhancement material, biochar can control cation exchange and hold onto nutrients in the soil, reducing nutrient leakage from soils. Additionally, Biochar activated with potassium hydroxide shows promise as a supercapacitor material.

The process of producing biochar involves a number of variables, including operational heat, gas flow rate, contact duration, pressure and ramp rate of furnace, all of which can affect the final product's production and quality [7]. The amount of the final product reduces as more volatiles eliminated from the structure during the breakdown of heavy hydrocarbons, which thought to be one of the major variables influencing the characteristics of biochar [8]. Research indicates that elevating the temperature during pyrolysis leads to a decrease in the yield of biochar [9]. This is to be expected that high temperature would trigger secondary reactions that completely disintegrate the char that forms at a lower temperature into aqueous and vapor phases, releasing more explosive components. The appropriate temperature for the creation of biochar requires careful consideration. While ash production at very high temperatures prevents the pore structure and surface area from expanding, higher temperatures encourage the creation of microspores and a better pore structure. [10]. In contrast, if the temperature is too low, the system may not be able to devolatilize volatile elements, which could lead to pores blockage and an underdeveloped pore network in the final product. This could result in negligible increases in pore volume and surface area [11].

According to earlier research, the ideal temperature range for the synthesis of biochar is 400–800 ℃. In order to increase the yield of biochar, secondary pyrolysis processes excluded and the risk of biomass thermal cracking reduced using a low heating rate [12]. Due to the melting of the biochar particles and the growth of both gaseous and liquid components, the amount of the finished product would be reduced at a very high heating rate. An inadequate heating rate also leads to accumulation inside the particles, obstructing pore entrances, because there is a short period for the volatile stuff to dissipate. [13], while depolymerization of biomass and the frequency of secondary pyrolysis reduce the yield of biochar and can reduce surface area [14]. An elevated level of volatile matter formation must avoid in order to prevent micro pore coalescence or the complete collapse of the carbon matrix. This eliminates the need for high heating rates; instead, an ideal range of 10-30 ℃/min recommended. Temperature, gas flow rate and heating rate all affect residence time. An abundant contact time is required for reaction in order to enhance biochar production and promote polymerization [15]. Nevertheless, a number of studies have found that yield is not directly correlated with residence time. Maximum pore volume for chemically activated biochar made from maize cobs has been reported to be produced by residence times ranging from 30 to 60 minutes; residence times ranging from 10 to 60 minutes have been observed to result in an increase in surface area [16]. Nevertheless, raise the lowered surface area even further.

Residence time is a crucial parameter to look at during the manufacture of biochar because of complications that arise from the interaction between it and other process parameters. Of particular relevance are residence times between 20 and 60 minutes. On the other hand, the impact of pressure on the creation of biochar is quite simple. Excessively high pressures cause spherical cavities to form and stop volatile stuff from escaping the system. Surface areas continuously decrease as pressure rises from 1 to more than 25 bar. The residence time of reaction elements can be lengthened by pressures somewhat higher than atmospheric pressure, aiding in the creation of char [17]. It also been proposed that the carbon concentration of the final product is pressure dependent. Vapors produced during pyrolysis, and if they are not removed from the system, they may interact with the char to change its properties [1]. Nitrogen is the supreme widely utilized carrier gas since it is more affordable and easily accessible than other inert gases. Carrier gases are employed in pyrolysis to provide an inert environment. The removal of vapors from the system, which prevents repolymerization, has been shown to slightly reduce the yield of biochar when gas flow rate is increased [19]. Previous research has demonstrated a yield reduction from 28.4 to approximately 27% when the nitrogen flow rate increased between 50 to 400 mL/min, with similar data for various systems suggest

that low to modest flow rates will generate a small impact on yield. Moderate gas flow rates from150 to 300 mL/min recommended for the best qualities because very high gas flowrates have shown to reduce biochar output and pore volume [20].

The association between process parameters and biochar performance has been the subject of previous research [21]. The limitations and incomplete knowledge of the combined influence of these variables on the biochar generated, however, exist. Different feedstock compositions, both physically and chemically, respond differently to operational conditions, resulting in a range of properties for the biochar produced. The selection of materials is a crucial stage in producing biochar. Climate conditions have the potential to influence parent material qualities [21]. The expense of acquiring the resource and turning it into customized supplies for the selected application should provide a fair return in order to guarantee practicability.

The native Pakistani wood used in this research work served as the raw materials, and screening tests helped distinguish between the widely accessible hard and soft wood. Using locally sourced raw materials offers the possibility of complexity in the production of char supplies for future uses, as well as a significant drop in the carbon imprint connected with supply or transportation. To learn more about the complementary impacts of particular process parameters on the characteristics of biochar and to guide the synthesis of biochar from such wood sources, this work used a design of experiments approach.

Experimental

Wood sample utilized in this work came from a Botanical Garden, University of Agriculture Faisalabad, Pakistan. Samples of wood included are Sitka spruce, radish purple cedar, Pak's pine, birch, oak and ash. A summary of the sample utilized in the study is given in Table-1. Sample 1 and 2 formed in order to compare the biochar made from hardwood and soft wood by using a design of experiments (DoE) approach. Samples 1 and 2 underwent screening tests to determine the kind of wood that will utilized in the DoE investigation. DoE was applied to sample 3 after the preliminary runs' findings on samples 1 and 2 were reexamined. Through parameter scoping, DoE runs were able to explore a larger parameter space. Minitab used to perform ANOVA (statistical analysis of variance) to identify the reactions resulting from numerous factors changing at once. This offers a more profound comprehension of the systematic aspects that affect the selected reactions statistically.

Table-1: Wood samples for the production of biochar.

Samples	Wood Type	Wood Species
1	Soft-Wood	Cedar, Sitka spruce, pine, oak, ash, and birch
2	Hard-Wood	Downey birch, oak, pine, Sitka spruce, and cedar
3	100% soft-wood	Pine, Sitka spruce and cedar

Design of Experiments (DoE)

DoE is a versatile method that aids in establishing a connection among input variables and a selected reaction. Depending on the situation, a system may employ several design types. Comparison uses t-test, Z-test and F-test to examine a single factor across various combinations. Factorial designs are used in variable screening to examine the impact of input variables on a systems or procedures overall performance. The examination of the link among pertinent input variables and the indicated output made possible by transfer function optimization. The transfer function used in system optimization to raise the system's overall performance. Lastly, the goal of resilient design is to lessen the effects of system variance without removing the underlying causes.

Rather than using the conventional one factor at a time method, this research work employed FFD (full factorial design), which categorized in variables selection, to evaluate potential interfaces of input variables. Three factors determined the screening runs: furnace temperature, flowrate of the activating gas, and contact time with the activating agent (CO_2). A survey of the literature led to the selection of two temperatures, 600 and 850 ℃, to investigate the differences in yields and the types of biochar that were formed. Thermal CO_2 activation is faster than chemical activation and enhances the sorption properties of biochar by forming new functional groups that produce a more homogeneous porous structure. We employed 100 or 250 mL/min flowrates with 20 and 60-minute residence periods.

Softwood shown to be a more attractive feedstock by screening; as a result, pure softwood samples were subjected to DoE (using FFD). For the FFD (full factorial design), Three variables were used, with an average temperature of 725 ℃: contact time interval (20 and 60 min), gas flow rate (100 and 250 mL/min), and the heating ramp rate (17 and 30℃). Full factorial design was created using Minitab, and as a result, there were 2^3 =8 studies overall for three elements, each with a setting for high and low. To

reduce the impact of uncontrollable circumstances, the runs were made randomly. In order to avoid wasteful material use and power consumption, center points excluded from the model. However, model still permitted to execute interaction up to the third order. The two design answers that were taken into consideration were surface area and biochar yield, since these attributes determine the biochar performance and economic viability.

Pyrolysis

The wood samples were cut into cubes with sides of around 5 cm before being burned. After being cleaned of dust with de-ionized water, these smaller cubes were oven dried for twenty-four hours at 100°C. A precursor weight of 30 ± 0.1g utilized for combustion. Four crucibles fitted with covers containing an equal distribution of the sample placed inside the Muffle Furnace, TMF-2100. Japan Eyela. A 250 mL/min CO_2 gas flow rate kept on the sample for 40 minutes in order to ensure an inert atmosphere. The furnace was also set to the proper temperature and dwell time. After that, heating initiated by adjusting the CO_2 gas flowrate to the values indicated in Table 2 and 3. After every run, the CO_2 gas flow rate stopped and the sample allowed to cool overnight once the furnace had reached room temperature.

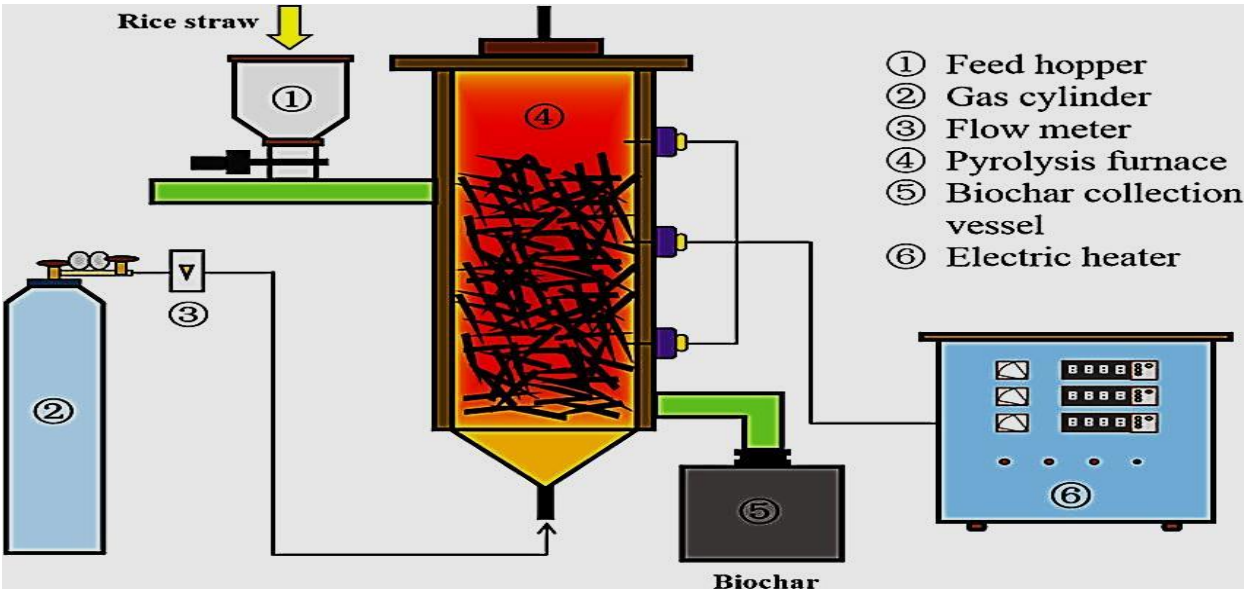

Fig. 1: A schematic representation of a muffle furnace.

Table-2: Physicochemical properties of Biochar produced using wood samples 1 and 2 (ramprate=17 °C/min).

Samples	CO_2 flow rate	Temp	Contact time (min)	Biochar weight	Yield (%)	Surface area	Microspore volume (cm3 /g)	Total pore volume (cm3 /g)	Average pore width
S1X	250(mL/min)	600°C	20	6.53g	21.8	544 (m2 /g)	0.18	0.27	3(nm)
S2X	250(mL/min)	600°C	60	6.21g	20.7	538 (m2 /g)	0.18	0.26	3(nm)
S3X	250(mL/min)	850°C	20	5.31g	17.7	597 (m2 /g)	0.21	0.28	3(nm)
S4X	100(mL/min)	850°C	60	4.40g	12.9	743 (m2 /g)	0.22	0.43	5(nm)
S5Z	250(mL/min)	600°C	20	7.58g	25.3	525 (m2 /g)	0.16	0.26	3(nm)
S6Z	250(mL/min)	600°C	60	6.95g	23.2	543 (m2 /g)	0.17	0.28	3(nm)
S7Z	250(mL/min)	850°C	20	5.15g	17.2	573 (m2 /g)	0.19	0.27	3(nm)
S8Z	100(mL/min)	60°C	100	4.53g	15.1	713 (m2 /g)	0.24	0.35	4(nm)

Table-3: Physicochemical properties of Biochar produced using wood sample 3.

Samples	CO_2 fow rate	Temp (°C)	Contact time (min)	Biochar weight	Yield (%)	Surface area (m2/g)	Micropore Volume (cm3/g)	Average pores width	Fixed carbon (%)	Volatie matter (%)
A1	250(mL/min)	710	60	5.30g	17.7	593	0.19	3(nm)	80.0	20.0
A2	100(mL/min)	710	60	5.27g	15.9	593	0.19	3(nm)	86.0	14.0
A3	250(mL/min)	710	20	6.08g	20.3	558	0.18	4(nm)	80.5	19.5
A4	100(mL/min)	710	20	6.31g	21.0	581	0.19	5(nm)	80.0	20.0
A5	250(mL/min)	710	60	4.40g	14.7	613	0.19	5(nm)	77.3	22.7
A6	100(mL/min)	710	60	3.65g	12.2	553	0.18	4(nm)	73.4	26.6
A7	250(mL/min)	710	20	6.08g	20.3	544	0.18	4(nm)	85.1	14.9
A8	100(mL/min)	710	20	6.07g	20.2	544	0.17	4(nm)	83.5	16.5

Fig. 1 shows the schematic layout for a muffle furnace that is used for pyrolysis.Samples allowed to come to room temperature before the total weight of the char was calculated.
Equation 1 is used to compute the sample's yield:

$$\textbf{Biochar yield}\ (\%) = \frac{\textbf{produced biochar weight (g)}}{\textbf{precursor weight (g)}} * 100 \quad (1)$$

Analysis and Characterization

Before analysis, samples of biochar crushed into a powder on a Micrometrics ASAP 2020 device utilizing nitrogen adsorption at 196°C. Degassing took place for 240 minutes at 200 °C (10 °C/min heating rate). The particular surface area and pore volume distributions of the samples were determined using the Brunauer-Emmett-Teller (BET) model [22].

Proximate Analysis

Representative Biochar samples were subjected to proximate analysis using thermogravimetry. The method used is very similar to the British Standard (BS1016) procedure [23]. A crucible containing 5–10 mg of crushed sample used for the Jupiter system's analysis. The crucible first heated to a temperature of 50 mL/min of nitrogen gas flow, and the initial mass recorded along with the mass that permitted to stabilize. After heating the sample to 120°C, it was given time to stabilize. Following the recording of the crucible mass, temperature raised to 920°C and maintained for three minutes prior to the mass reading taken. At last, temperature lowered to 820°C, and feeding gas was replaced with compressed air at a rate of 50 mL/min.

Scanning Electron Microscopy (SEM)

The structural properties of the biochar surface captured using SEM. A little solid piece removed from a charcoal cube and inserted into the device (Tungsten low-vacuum JEOL JSM-IT100 SEM). Images were taken at 10 µm with a magnification of ×1000. There was a 20 kV voltage differential while the beam current remained constant at 35.

Point Zero Charge (PZC)

PZC analysis carried out using the salt addition method [24]. adjusting a 40 mL 0.1 M NaNO3 sample to five different pH values ranging from 3 to 11.To get the right pH, solution of 0.1 M HCl and 0.1 M NaOH utilized. The beaker filled with 0.2g of crushed biochar and stirred for 24 hours at 450 rpm. The pH of the permeate was determined after the final solution was filtered. Calculating the difference between the samples' initial and final pH values plotting the pH change versus the starting value helped me discover the PZC.

Result and Discussion

Minitab Results and Analysis of Regression

The data set from the DoE runs analyzed using Minitab. Following Eqs. 2 and 3 are the regression equation for the two responses, yield (Y^a) or surface area (Y^b). A step-by-step methodology that combines forward selection and backward exclusion processes was employed for the factorial design study. The forward selection approach determines the variables to include in a model. Additional variables in forward selection not ever eliminated. On the other hand, terms with the smallest modified sum of squares eliminated from the original model using the backward elimination process. Values for "Alpha to enter" and "Alpha to remove" used to decide whether to add or remove a variable from model. A variable kept in model if its *p* value is smaller than the value designated as "Alpha to enter," and vice versa. The system default for both alpha values in this investigation was set to 0.15.

$$\text{Yield } (Y^a) = 6.20 + 0.0058\ A + 0.0300\ C - 0.001900\ A\ C \quad (2)$$

$$\text{Surface area } (Y^b) = 577.8 + 1.031\ \text{Contact time} - 1.85\ \text{ramp rate} \quad (3)$$

where C is the ramp rate measured in °C/min and A is the contact time measured in min.

Be aware that variable B (gas flow rate) did not show any significant results. For equations 2 and 3, the coefficient of determination (R^2) stayed equal to 0.95 and 0.70, correspondingly. According to the values, model can account for more than 95% and 70%, respectively, of the fluctuations in the surface area and yield responses. Additionally, the model shows that variations in the activating gas's flow rate do not appear to have a significant impact on the obtained results. Pareto chart of the standardized effects of variable on the response displayed in Fig. 2.

Analysis of Variance (ANOVA)

The input variables include ramp rate, contact time, and flow rate statistically analyzed in order to determine whether there were any single or combined effects on the selected answers. The ANOVA table created in Minitab's *p* values and F values that can be used as a means of assessing the model's suitability.

Table 4 presents the data generated for surface area and yield. A model must have a high F value and a *p* value less than the significant level, which in this instance is 0.05 for a 95% confidence interval, in order to considered significant [25]. The models are significant in both circumstances, with the yield model being significantly more accurate than the surface area regression when the *p* value for model is lower than 0.05. Table shows that ramp rate and contact duration have decisive influence on yield, with the furnace contact time, which has F value of 56.8, serving as the primary influencing factor. Additionally, here is a noticeable bidirectional relationship on yield among contact time (min) and heating ramp rate(°C). Moreover, model indicates that the CO_2 gas flow rate has no effect on the yield of char. It was projected that contact time alone would be the influencing variable for biochar surface area. The heating ramp rate *p* value was greater than 0.05, indicating that this variable is not substantial in determining surface area. There was no anticipated impact of CO_2 gas flow rate on surface area.

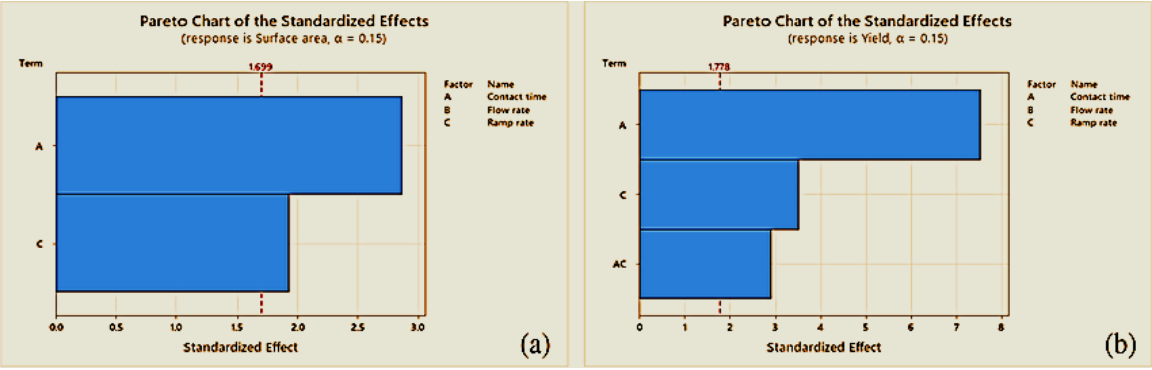

Fig. 2: Pareto chart showing the effects of variables on both (a) surface area or (b) yield.

Table-4: Analysis of variance findings for surface area and yield.

Findings for Yield					
Source	**DF**	**Adj SS**	**Adj MS**	***F* value**	***p* value**
Model	**3**	**5.9828**	**1.99426**	**25.87**	**0.004**
Linear	**2**	**5.3331**	**2.66650**	**34.61**	**0.003**
Contact time	**1**	**4.3807**	**4.38080**	**56.85**	**0.002**
Ramp rate	**1**	**0.9522**	**0.95220**	**12.36**	**0.025**
Error	**4**	**0.3081**	**0.07704**		
Total	**7**	**6.2910**			
Findings for Surface area					
Model	**2**	**4943**	**2471.7**	**5.97**	**0.048**
Linear	**2**	**4943**	**2471.7**	**5.96**	**0.048**
Contact time	**1**	**3403**	**3403.1**	**8.20**	**0.035**
Ramp rate	**1**	**1540**	**1540.1**	**3.72**	**0.112**
Error	**5**	**2075**	**414.8**		
Total	**7**	**7018**			

Optimisation of Response

Minitab used to create an optimized response with the aim of maximizing both of the chosen responses, taking into account that model was statistically significant in terms of surface area and yield. Minitab's suggested solution produced surface area of 593 m^2/g and a yield of 5.3g with a contact period of 60 min and heating ramp rate of 17°C, with no specified value for the gas flow rate. 78 % of the generated solution was deemed desirable. Experiments A1 and A2, which were conducted with different flow rates and a contact period of 60 minutes and a ramp rate of 17 °C/min, had already included the proposed solution. In both instances, the surface area experimental values that were noted were 593 m^2/g. Furthermore, both samples yield was roughly 5.3g, which is in excellent agreement with the theoretical expectations. Although the theoretical and experimentally acquired results are closely related, because surface area regression is not very accurate, more research is needed to determine how parameters affect the characteristics of biochar. It is possible to enhance the model by running center points; however, it's necessary to reduce experimental runs to bolster the concept and stop resource utilization of durability. Further analysis of the biochar characterization data and its correlation with the original input process variables was done in the ensuing sections.

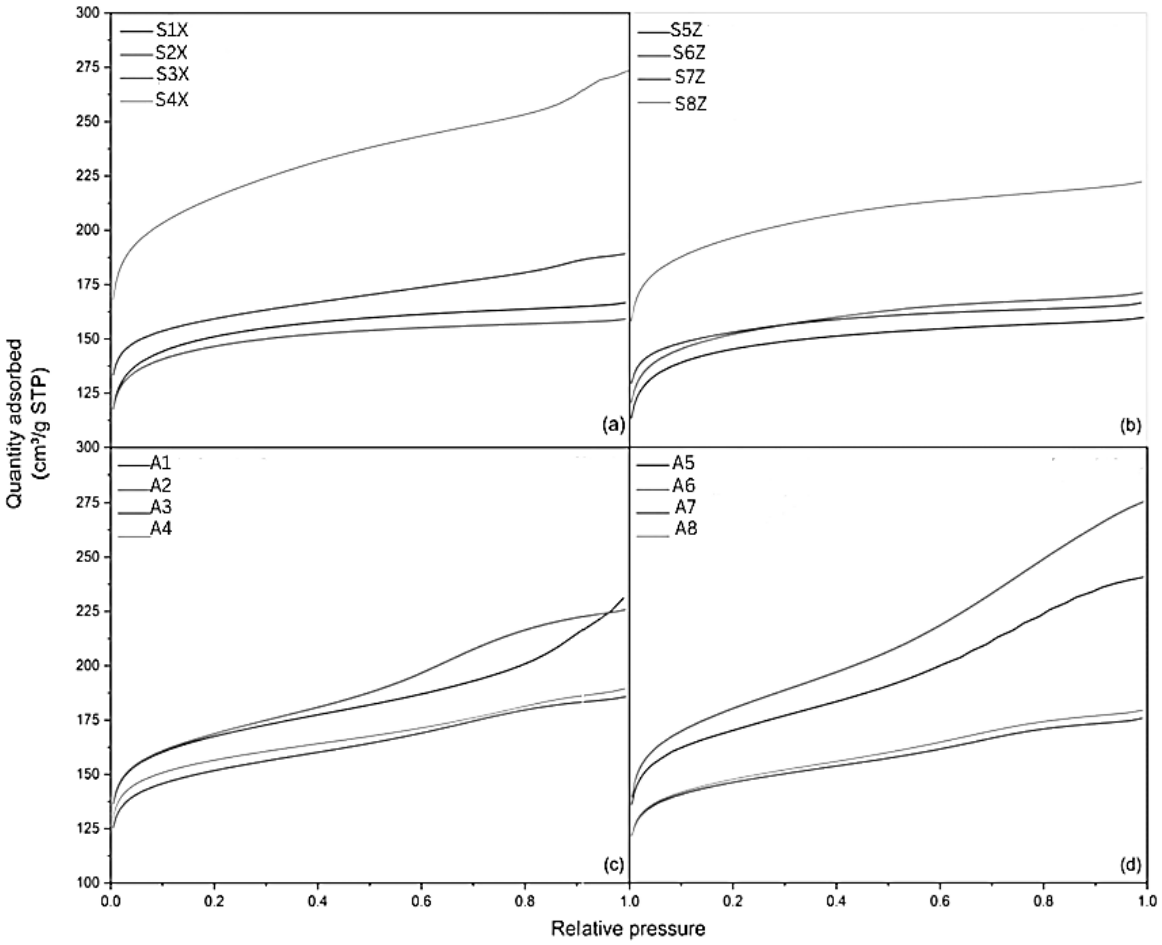

Fig. 3: Adsorption isotherms obtained for biochar samples.

Yield of Biochar

Table-2 displays the yield (%) of biochar generated by selected wood samples SX or SZ at various temperatures and operating conditions during the process of biochar production. The yield trend is as anticipated: lesser amounts of generated biochar are produced at higher pyrolysis temperatures [26].

The mass of the biochar increases as the temperature rises as more volatiles eliminated from the system, which lowers the biomass in the system. It is clear that a direct combination of the operational constraints determines the results. The maximum biochar yield of 6.5g obtained from the softwood chars (Samples SX) at a high gas federate of 250 mL/min, a low contact time period of 20 min, and a pyrolysis temperature of 600°C. A slight decrease in yield of less than 1% was seen when the contact duration was extended to 60 minutes while the other two parameters remained same. The findings imply that the increase in contact time from 20 to 60 minutes has no appreciable effect on the yield of the product. The hardwood chars (samples SZ) showed a similar pattern. Low contact duration period, low pyrolysis temperature and high gas flowrate were used to get a 7.6g of maximum yield. A 2% drop in yield was seen with an increase in contact duration. At 850°C, low gas yield rate, and 60-minute residence duration, the lowest yield achieved. Hardwood samples outperformed softwood samples in terms of yields under comparable conditions. For trial S1X, the soft wood yield was 21.8%, and the hard wood biochars were 25.3% in comparable factors (S5Z). For the other runs in each of the two wood batches, the yield difference was not very significant. This finding, along with the precise surface areas measured, suggested that all 100% of the softwood samples merited more study.

Yield of biochar produced during DoE runs is shown in Table 3. The heating ramp rate maintained at 17°C/min and the temperature in A1-A4 fixed at 725°C, which was the mean of the two selected temperatures. An average yield of about 17.5%

obtained after 60 minutes of contact with both gas flowrates. Reducing the contact duration to 20 minutes resulted in a minor improvement in yield, giving about 20%. With a high contact time and a heating ramp rate of 30°C/min for A5-A8, yield significantly decreased for runs [27]. However, the yield with shorter residence durations did not appear to be affected by the high heating rate. According to the findings, temperature appears to be the main factor influencing biochar output. The yield is clearly influenced by contact time duration and ramp rate, but gas flow rate has no appreciable effect, as the prior Minitab output demonstrated.

Characterization of Porous Structures

Adsorption isotherms found in the screening investigation are displayed in Figs 3a and 3b. Type-II isotherm driven by adsorption over microporous materials is shown by Experiments S1X to S4X. The hardwood samples from tests S5Z-S8Z likewise show a strong uptake at first, which is followed by a plateau. High relative pressure appears to cause a little amount of final absorption, which explained by type-II isotherm and multilayered adsorption [28]. DoE biochar adsorption isotherms, which are shown in Figs. 3c and d, show a more prevalent form of II/IVa isotherm behavior featuring substantial uptakes at first [29]. For the pure soft wood sample (sample 3) in the later studies, mesoporous nature is generally more evident.

Table 2 displays the textural data obtained for the screening samples that includes the average pore widths, surface area, micro pores and total pore volumes. Table 3 provides similar data on DoE samples. Equation 4 utilized to ascertain the samples' total pore volume (TPV).

$$TPV = (QSat * MW/Vm)/\rho liq \quad (4)$$

QSat is the nitrogen adsorption at maximum, expressed in cm^3/g, is typically achieved at a relative pressure of 0.97 or higher.

MW is the weight of N_2 (28 g/mol).

Vm is the volume (22.4 L) that one mol of gas occupies.

ρliq=the liquid N2's density (808 g/L) at boiling point.

The t plot method put forward by Lippens and Boer used to determine the micropore volumes showed in Tables 2 and 3[30]. It concluded that micro porosity increased as pyrolysis temperatures increased. The samples with lower gas federates and longer residence durations have the largest ratio of micro pore volume to TPV. V(micropore) / V(total ratios) for studies with 20-minute hold duration at a high temperature are comparable for high gas flows. The available data indicates that the development of micro porosity and residence time are inversely correlated. Optimization of micro porosity can be beneficial for interactions between adsorbents and tiny adsorbate species. DoE tests A5 and A6 suggest that increasing the ramp rate and holding the biochars longer can improve their mesoporous character, which has been demonstrated to be beneficial for the applications in aqueous phase [31]. BET analysis used to calculate surface areas; however, this type of examination is very sensitive to the relative pressure ranges that is chosen, especially for microporous materials [32]. Rouquerol *et al.*, 2007 proposed four-consistency criteria that can be used to determine the ideal relative pressure range [33].

1) The range that only shows a monotonic increase in the product of the relative pressure 1 minus and the adsorbate-loading rate should be selected.
2) BET "C constant" value needs to be positive. C constant is associated with the energetics of the first adsorbed layer in adsorption and measures the interactions between the adsorbents and adsorbate [32].
3) The specified linear region should have the monolayer loading that corresponds to the relative pressure.
4) The relative pressure found in criteria 3 ought to match the value obtained from BET theory in accordance with surface loading with a tolerance of 20%.

All of the samples created for this investigation underwent the Rouquerol adjustment due to the substantial micro porosity that was noted in Tables 2 and 3. The maximum BET surface area was measured using softwood precursor (S4X) at 850°C pyrolysis temperature, 100 mL/min gas flowrate, and 60 minutes residence time. Biochar formed with similar conditions but with longer hold times have higher surface areas than those produced by shorter residence times. A prior research [34] detailed comparable observations of increased surface areas with residence time. Biochar with larger surface areas generally created by pyrolysis operations carried out at 725°C. Additionally, the middle temperatures provided a fair trade-off between average pore widths and biochar output. It can deduce that for DoE runs, smaller ramp rates with larger residence times are directly related to surface area. These samples' decreased Vmicropore/Vtotal ratio also points to a more visibly porous structure. Compared to other

wood based biochar described in the literature, 100% softwood chars yielded the greatest biochar surface areas [12 35]. Similar to yield, surface area measurements used to complement the Minitab output. Only exemption is in experiment A6, where a fast ramp rate has led to decrease in the surface area of biochar. This result might relate to the model's decreased accuracy. The Barrett-Joyner-Halenda (BJH) analytical data on pore width (Tables 2 and 3) further supports the biochar predominately microporous character. The runs with high ramp rates at 725℃ had the biggest average pore diameters. As already mentioned, shorter hold times led to both smaller pore widths and higher micro porosity. Preponderantly softwood biochar (S1X-S4X) were practically as microporous as hardwood biochar (S5Z-S8Z), and sample 3 (exclusively softwood, A1-8) demonstrated the highest meso porosity. The outcomes suggest that sample 1 may find use in the gas phase for the adsorption of tiny adsorptive species, including carbon capture.

Proximate Analysis

Table 3 reports the dry ash compositions of the feedstock and DoE biochar as determined by thermogravimetric analysis. The samples underwent dry treatment to eliminate fluctuations in moisture contents, and ash free treatment to address variations in inorganic forms derived from the natural precursors. In trials A1 and A2, a high contact time led to an 80% fixed carbon contents and a= 20% volatile matter contents. Compared to the feedstock's fixed carbon contents of 20.3%, there was a noticeable rise. In experiment A2, the carbon contents rose to 86% and the volatiles lowered to 14% with a significantly lower gas flowrate [36]. The volatile fractions and fixed carbon in tests A3 and A4, which had shorter residence times, were not significantly affecting by gas flowrates.

Volatile matter accumulates because of high heating rates and extended residence times. This assertion corroborated by the results obtained in A5 and A6, which show increased volatile content and carbon percentages below 80 compared to their lower heating ramp rate counterparts. The percentage of volatiles decreased significantly with a shorter hold duration (A7 and A8), and there was a favorable effect on the fixed carbon content. The main factor influencing fixed carbon and volatiles found to be residence time, with fluctuations brought on by fluctuating gas flow rates being essentially insignificant.

The findings suggest that, albeit there would be a noticeable yield loss, a faster ramp rate in conjunction with a shorter residence time could result in biochar with the maximum fixed carbon contents and the lowest volatile portion.

Scanning Electron Microscopy

The SEM pictures for biochar samples with lower ramp rates displayed in Figs 5a–d, while the observations for biochar with greater ramp rates displayed in Figs 5e–g. In both low and high ramp rate samples, a well-developed pore network is evident. The photos at 10µm and 1000-×magnification indicate that the parent material's complex network of pores exposed by the high pyrolysis temperatures [37]. It takes a sufficiently high pyrolysis temperature to remove the outer layer of biochar. Decreased ash content may be the cause of the open nature of the pores, which lowers the chance of clogging. Different ramp rates did not appear to have any effect on the pore network that emerged in biochar samples.

Point Zero Charge (PZC)

Surface functional groups and material origin appear to have a greater influence on the surface charge of the biochars generated under various operational conditions than selected DoE variables. The samples in this investigation had an average PZC of 7.20±0.01. pH of wood-based biochar is influenced by pyrolysis temperatures. Elevated temperatures cause the loss of acidic functional groups such carboxylic and phenols in addition to volatile materials, which increases the alkaline surface charge [38]. For instance, slow pyrolysis action of wood based pellets at 200℃ created biochar with pH 4.6. While increasing the temperature to 600℃, the consequential biochar had a pH of 9.5. Biochar with pH (H_2O) of 8.58±0.01 were used in a comparable observation on wood chips biochar that were pyrolyzed at 500℃ [39]. Targeting anionic species from effluents with a slightly alkaline surface charges may find use in drinking water system that run in an acidic environment with little alteration.

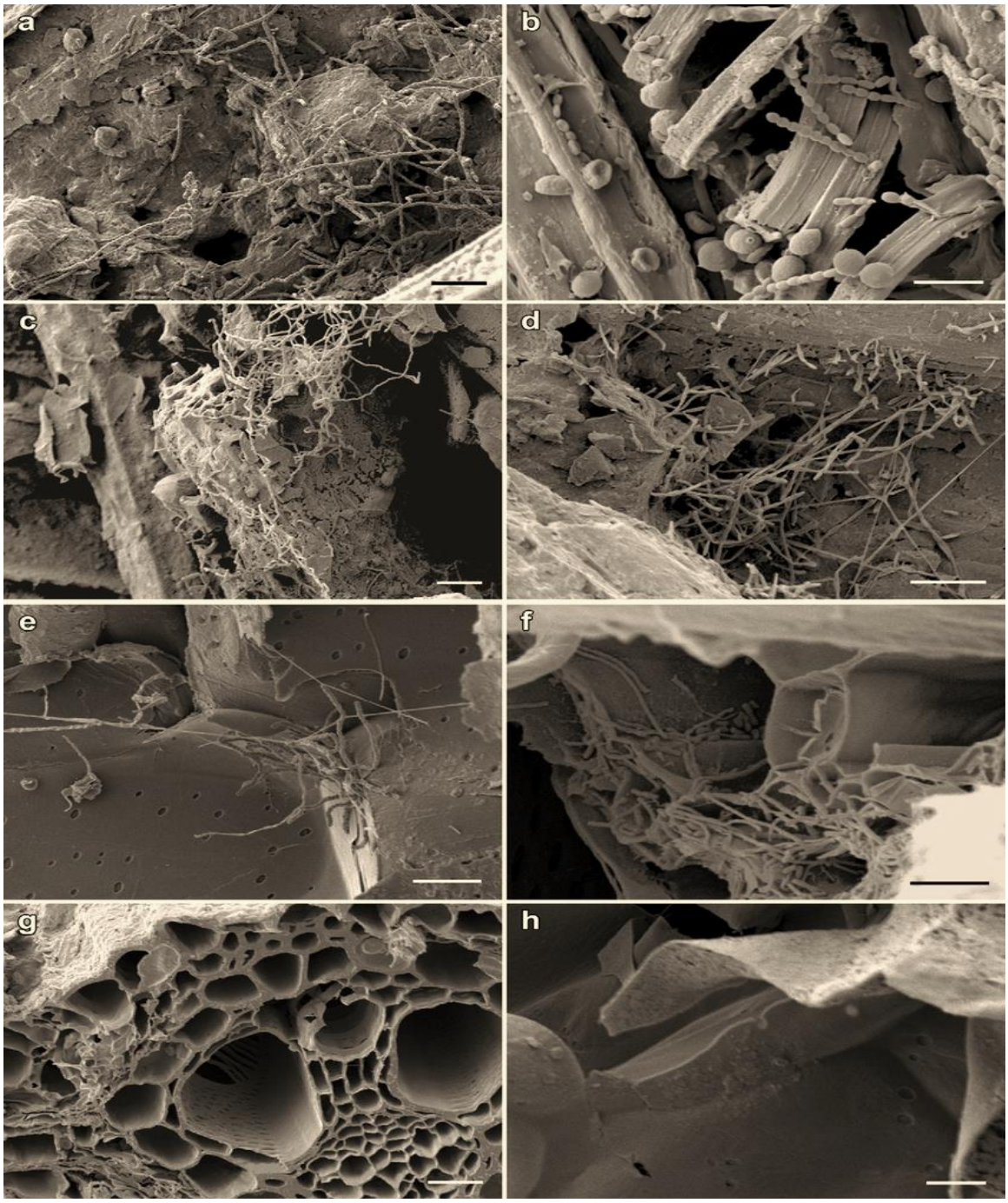

Fig. 5: Samples of biochar with lower ramp rate (a–d SEM); samples of biochar with greater ramp rate (e–h SEM).

Result and Discussion

Analyzing the diverse array of outcomes acquired for the charcoals generated in this investigation indicates a noteworthy association between the characteristics of biochar and the parameters employed in its creation. Compared to a subset of biochar described in the literature [34 39], the biochar surface areas that this study reports are larger. Similar to the DoE biochar, the quantity of fixed carbon in wood made biochar seems to be constant at about 80%. It has been reported that structures that are beyond 400°C become recalcitrant due to the disappearance of alkyl and carboxylic

groups and volatile substances [40]. SEM pictures also show the carbonaceous skeletons pores arranged in a concentric pattern. It has also been noted that biochars' alkalinity increases at higher temperatures [35]. The average PZC of the DoE biochar in this investigation was found to be 7.20±0.01. The biochars' contact angle research revealed a hydrophilic nature in addition to a neutral pH. The biochar produced in this experiment is highly surface-aread and highly carbon-rich., and are hydrophilic, which means that they have a great deal of potential for application in systems that treat wastewater [41]. According to the DoE study, the influence of process parameters on the characteristics of biochar seems to be substantial and may offer a technique to create sustainable biochar tailored to particular uses.

Conclusion

This study investigates the design of experiments on Pakistani wood biochar and examines the impact of process constraints on its characteristics. The findings highlight that process parameters, such as temperature and time, significantly influence the biochar's surface area, pore volume, and overall quality. The results suggest that optimizing these factors can enhance biochar production, making it more suitable for various applications.

References

1. B. Saleem, M. K. Ali and C. H. Khan, Natural Inhibitors for Inhibiting the Production of Aflatoxins, *J. Nat. Prod*., **57,** 1422 (2000).
2. J. Lee, K-H. Kim and E. E. Kwon, Biochar as a Catalyst. Renewable and Sustainable *Energy* Reviews.,**77**, 70 79 (2017).
3. W-J. Liu, H. Jiang and H-Q. Yu, Emerging applications of biochar-based materials for energy storage and conversion. *Energy Environ Science*., **12**, 1751 1779 (2019).
4. [M. Ahmad, A. U. Rajapaksha and J. E. Lim, Biochar as a sorbent for contaminant management in soil and water: A review. *Chemosphere.*, **99**, 19 33 (2014).
5. J. Ahmad, F. Patuzzi and T. D. U. Rashid, Exploring untapped efect of process conditions on biochar characteristics and applications. *Environ Technol Innov*., **21**, 101310 (2020).
6. A. M. Dehkhoda, A. H. West and N. Ellis, Biochar based solid acid catalyst for biodiesel production. *Applied Catalysis A: General*., **382**, 197 204 (2010).
7. B. Inan, A. T. Kocer and D. B. Ozçimen, Valorization of lignocellulosic wastes for low-cost and sustainable algal biodiesel production using biochar-based solid acid catalyst. *Journal of Analytical and Applied Pyrolysis*., **173**, 106095 (2023).
8. A. A. Boateng, M. Garcia-Perez, O. Masek, R. Brown and B. del Campo, Biochar production technology. In *Biochar for environmental management*, p. 63-87 (2015).
9. Q. He, L. Ding, A. Raheem, Q. Guo, Y. Gong and G. Yu, Kinetics comparison and insight into structure-performance correlation for leached biochar gasification. *Chemical Engineering Journal*., **417**, 129331 (2021).
10. A. Tomczyk, Z. Sokołowska and P. Boguta, Biochar physicochemical properties: pyrolysis temperature and feedstock kind effects. *Reviews in Environmental Science and Bio/Technology*., **19**, 191 215 (2020).
11. J. A. Ippolito, L. Cui, C. Kammann, N. Wrage-Monnig, J. M. Estavillo, T. Fuertes-Mendizabal and N. Borchard, Feedstock choice, pyrolysis temperature and type influence biochar characteristics: a comprehensive meta-data analysis review. *Biochar*., **2,** 421 438 (2020).
12. K. L. Martinez-Mendoza, J. M. Barraza-Burgos, N. Marriaga-Cabrales, F. Machuca-Martinez, M. Barajas and M. Romero, Production and characterization of activated carbon from coal for gold adsorption in cyanide solutions. *Ingeniería e Investigacion*., **40,** 34 44 (2020).
13. H. J. Huang, Y. C. Chang, F. Y. Lai, C. F. Zhou, Z. Q. Pan, X. F. Xiao and C. H. Zhou, Co-liquefaction of sewage sludge and rice straw/wood sawdust: The effect of process parameters on the yields/properties of bio-oil and biochar products. *Energy.*, **173**, 140 150 (2019).
14. A. Y. Elnour, A. A. Alghyamah, H. M. Shaikh, A. M. Poulose, S. M. Al-Zahrani, A. Anis and M. I. Al-Wabel, Effect of pyrolysis temperature on biochar microstructural evolution, physicochemical characteristics, and its influence on biochar/polypropylene composites. *Applied sciences*., **9,** 1149 (2019).
15. B. Zhao, D. O'Connor, J. Zhang, T. Peng, Z. Shen, D. C. Tsang and D. Hou, Effect of pyrolysis temperature, heating rate, and residence time on rapeseed stem derived biochar. *Journal of Cleaner Production*., **174**, 977 987 (2018).
16. H. B. Kim, J. G. Kim, T. Kim, D. S. Alessi and K. Baek, Interaction of biochar stability and abiotic aging: Influences of pyrolysis reaction medium and temperature. *Chemical Engineering Journal*., **411**, 128441 (2021).
17. K. Crombie, O. Masek, S. P. Sohi, P. Brownsort and A. Cross, The effect of pyrolysis conditions on biochar stability as determined by three methods. *Gcb Bioenergy*., **5,** 122 131 (2013).

18. [S. Wang, H. Zhang, H. Huang, R. Xiao, R. Li and Z. Zhang, Influence of temperature and residence time on characteristics of biochars derived from agricultural residues: A comprehensive evaluation. *Process Safety and Environmental Protection*., **139**, 218 229 (2020).
19. L. Qin, Y. Wu, Z. Hou and E. Jiang, Influence of biomass components, temperature and pressure on the pyrolysis behavior and biochar properties of pine nut shells. *Bioresource Technology*., **313,** 123682 (2020).
20. N. Mahinpey, P. Murugan, T. Mani and R. Raina, Analysis of bio-oil, biogas, and biochar from pressurized pyrolysis of wheat straw using a tubular reactor. *Energy & Fuels*., **23**, 2736-2742 (2009).
21. C. Bouchelta, MS. Medjram, m. Zoubida, Efects of pyrolysis conditions on the porous structure development of date pits activated carbon. *J Anal Appl Pyrolysis*., **94**, 215 222 (2012).
22. M. Hassan, Y. Liu R. Naidu, Infuences of feedstock sources and pyrolysis temperature on the properties of biochar and functionality as adsorbents: a meta-analysis. *Science of The Total Environment*., **744**, 140714 (2020).
23. S. Brunauer, PH. Emmett, E. Teller, Adsorption of gases in multimolecular layers. *J Am Chem Soc*., **60,** 309 319 (1938).
24. S. S. J. Warne, Proximate analysis of coal, oil shale, low quality fossil fuels and related materials by thermogravimetry. *TrAC Trends in Analytical Chemistry*., **10**,195 199 (1991).
25. E. N. Bakatula, D. Richard, CM. Neculita, GJ. Zagury, Determination of point of zero charge of natural organic materials. *Environ Sci Pollut Res*., **25**, 7823 7833 (2018).
26. E. H. El-Masry, H. A. Ibrahim, O. A. Abdel Moamen and W. F. Zaher, Sorption of some rare earth elements from aqueous solutions using copolymer/activated carbon composite: multivariate optimization approach. *Advanced Powder Technology*., **33**, 103467 (2022).
27. G. A. Idowu and A. J. Fletcher, The manufacture and characterisation of rosid angiosperm-derived biochars applied to water treatment. *Bioenergy Res*., **13**, 387 396 (2020).
28. L. Leng, Q. Xiong, L. Yang, An overview on engineering the surface area and porosity of biochar. *Science of The Total Environment*., **763**, 144204 (2021).
29. R. Muzyka, E. Misztal, J. Hrabak, S. W. Banks and M. Sajdak, Various biomass pyrolysis conditions influence the porosity and pore size distribution of biochar. *Energy.*, **263,** 126128 (2023).
30. M. Thommes, K. Kaneko, AV. Neimark, Physisorption of gases, with special reference to the evaluation of surface area and pore size distribution (IUPAC Technical Report). *Pure Appl Chem*., **87**, 1051 1069 (2015).
31. B. C. Lippens and J. H. de Boer, Studies on pore systems in catalysts: V. The t method. *J Catal*., **4,** 319 323 (1965).
32. M. Parsa, M. Nourani, M. Baghdadi, Biochars derived from marine macroalgae as a mesoporous by-product of hydrothermal liquefaction process: characterization and application in wastewater treatment. *Journal of Water Process Engineering.*, **32**, 100942 (2019).
33. D. A. Gomez-Gualdron, P. Z. Moghadam, J. T. Hupp, Application of consistency criteria to calculate BET areas of microand mesoporous metal–organic frameworks. *J Am Chem Soc*., **138**, 215 224 (2016).
34. J. Rouquerol, P. Llewellyn and F. J. S. S. S. C. Rouquerol, Is the BET equation applicable to microporous adsorbents. *Stud. Surf. Sci. Catal.*, **160**, 49 56 (2007).
35. J. Zhang, J. Liu and R. Liu, Effects of pyrolysis temperature and heating time on biochar obtained from the pyrolysis of straw and lignosulfonate. *Bioresource Technology.*, **176,** 288 291 (2015).
36. S. Jiang, T. A. Nguyen, V. Rudolph, H. Yang, D. Zhang, Y. S. Ok and L. Huang, Characterization of hard-and softwood biochars pyrolyzed at high temperature. *Environmental geochemistry and health.*, **39,** 403 415 (2017).
37. L. Luo, C. Xu, Z. Chen, S. Zhang, Properties of biomassderived biochars: combined efects of operating conditions and biomass types. *Bioresour Technol*., **192**, 83 89 (2015).
38. BC. Chaves Fernandes, K. Ferreira Mendes, AF. Dias Junior, Impact of pyrolysis temperature on the properties of eucalyptus wood-derived biochar. *Materials.*, **13,** 5841 (2020).
39. SM. Shaheen, NK. Niazi, E. Noha, Wood-based biochar for the removal of potentially toxic elements in water and wastewater: a critical review. *Int Mater Rev.*, **64**, 216 247 (2019).
40. M. Pipiska, EK. Krajcikova, M. Hvostik, Biochar from wood chips and corn cobs for adsorption of thiofavin t and erythrosine B. *Materials*., **15**, 1492 (2022).
41. P. Campos, A. Z. Miller, H. Knicker, M. F. Costa-Pereira, A. Merino and J. M. De la Rosa, Chemical, physical and morphological properties of biochars produced from agricultural residues: Implications for their use as soil amendment. *Waste Management*., **105**, 256 267 (2020).
42. W. Xiang, X. Zhang, J. Chen, W. Zou, F. He, X. Hu and B. Gao, Biochar technology in wastewater treatment: A critical review. *Chemosphere*., **252**, 126539 (2020).